Acta Biomaterialia 54 (2017) 212–226

Contents lists available at ScienceDirect

Acta Biomaterialia

journal homepage: www.elsevier.com/locate/actabiomat

Full length article

Thermally triggered hydrogel injection into bovine intervertebral disc tissue explants induces differentiation of mesenchymal stem cells and restores mechanical function

A.A. Thorpe [a], G Dougill [b], L. Vickers [a], N.D. Reeves [b], C. Sammon [d], G. Cooper [c], C.L. Le Maitre [a,*]

[a] Biomolecular Sciences Research Centre, Sheffield Hallam University, S1 1WB, UK
[b] Faculty of Science & Engineering, Manchester Metropolitan University, M1 5GD, UK
[c] School of Mechanical, Aerospace and Civil Engineering, University of Manchester, M13 9PL, UK
[d] Materials and Engineering Research Institute, Sheffield Hallam University, S1 1WB, UK

ARTICLE INFO

Article history:
Received 15 November 2016
Received in revised form 20 February 2017
Accepted 7 March 2017
Available online 8 March 2017

Keywords:
Intervertebral disc
Nucleus pulposus
Injectable hydrogel
Mesenchymal stem cells
Tissue explant culture

ABSTRACT

We previously reported a synthetic Laponite® crosslinked pNIPAM-co-DMAc (L-pNIPAM-co-DMAc) hydrogel which promotes differentiation of mesenchymal stem cells (MSCs) to nucleus pulposus (NP) cells without additional growth factors. The clinical success of this hydrogel is dependent on: integration with surrounding tissue; the capacity to restore mechanical function; as well as supporting the viability and differentiation of delivered MSCs. Bovine NP tissue explants were injected with media (control), human MSCs (hMSCs) alone, acellular L-pNIPAM-co-DMAc hydrogel or hMSCs incorporated within the L-pNIPAM-co-DMAc hydrogel and maintained at 5% O_2 for 6 weeks. Viability of native NP cells and delivered MSCs was maintained. Furthermore hMSCs delivered via the L-pNIPAM-co-DMAc hydrogel differentiated and produced NP matrix components: aggrecan, collagen type II and chondroitin sulphate, with integration of the hydrogel with native NP tissue. In addition L-pNIPAM-co-DMAc hydrogel injected into collagenase digested bovine discs filled micro and macro fissures, were maintained within the disc during loading and restored IVD stiffness. The mechanical support of the L-pNIPAM-co-DMAc hydrogel, to restore disc height, could provide immediate symptomatic pain relief, whilst the delivery of MSCs over time regenerates the NP extracellular matrix; thus the L-pNIPAM-co-DMAc hydrogel could provide a combined cellular and mechanical repair approach.

Statement of Significance

Low back pain (LBP) is associated with degeneration of the intervertebral disc (IVD). We have previously described development of a jelly delivery system (hydrogel). This has the potential to deliver adult stem cells to the centre of the IVD, known as the nucleus pulposus (NP). Here, we have demonstrated that adult stem cells can be safely injected into the NP using small bore needles, reducing damage to the disc. Following injection the hydrogel integrates with surrounding NP tissue, promotes differentiation of stem cells towards disc cells and restores IVD mechanical function. The hydrogel could be used to restore mechanical function to the IVD and deliver cells to promote regeneration of the disc as a minimally invasive treatment for LBP.

1. Introduction

Low back pain (LBP) is an increasingly prevalent clinical condition that affects over 80% of the population at some point during their lifetime [1]. The aetiology of chronic LBP is thought to be multifactorial; however, degeneration of the intervertebral disc (IVD) is regarded as a key attributing factor [2,3]. Morphologically the IVD can be divided into three distinct regional structures: the cartilaginous endplates (CEP); the annulus fibrosus (AF) and the central gelatinous nucleus pulposus (NP), rich in proteoglycans

Abbreviations: LBP, low back pain; IVD, intervertebral disc; CEP, cartilaginous end plate; AF, annulus fibrosus; NP, nucleus pulposus; ECM, extracellular matrix; MSCs, mesenchymal stem cells; hMSCs, human mesenchymal stem cells; L-pNIPAM-co-DMAc, laponite® crosslinked pNIPAM-co-DMAc hydrogel; FCS, fetal calf serum; NIPAM, N-isopropylacrylamide; DMAc, N,N′-dimethylacrylamide; AIBN, 22′-azobisisobutyronitrile; SEM, scanning electron microscopy; IHC, immunohistochemistry.

* Corresponding author.
E-mail addresses: abbey.a.thorpe@student.shu.ac.uk (A.A. Thorpe), g.dougill@mmu.ac.uk (G Dougill), hwblv1@exchange.shu.ac.uk (L. Vickers), n.reeves@mmu.ac.uk (N.D. Reeves), c.sammon@shu.ac.uk (C. Sammon), glen.cooper@manchester.ac.uk (G. Cooper), c.lemaitre@shu.ac.uk (C.L. Le Maitre).

http://dx.doi.org/10.1016/j.actbio.2017.03.010
1742-7061/

(mainly aggrecan) and collagen type II [4]. The IVD transmits load, facilitates a range of spinal movement and dissipates energy during motion [5].

Degeneration of the IVD is characterised by a number of progressive extracellular matrix (ECM) changes including altered matrix synthesis and increased degradation of normal matrix components [6], resulting in an overall reduction in the proteoglycan content of the NP [7]. This is mediated by the catabolic phenotype of degenerate NP cells [8,9] alongside decreased viability as well as increased apoptosis [17] and senescence of remaining NP cells [10]. This results in reduced NP tissue hydration and an overall loss in disc height [11], culminating in mechanical failure resulting in abnormal stresses to surrounding spinal tissues and compression of nerve routes [12]. Consequently, the restoration of disc height is a key therapeutic target for the symptomatic relief of chronic LBP.

New approaches in tissue engineering have led to the investigation of a variety of treatment options aimed at the restoration of disc height using acellular implants [13–16], the use of regenerative cells [17–20] or the combined delivery of regenerative cells with supporting mechanical scaffolds [21,22]. Mesenchymal stem cells (MSCs) have been highlighted as an attractive cell choice since they have proliferative capacity, can be extracted from a variety of adult tissues and have the capacity to differentiate into NP like cells [19,20,23–25]. However, concerns remain regarding MSC leakage [26], as well as a lack of control over differentiation following injection [27], thus highlighting the potential need for cell carrier systems. The use of a combined approach is appealing, since it is hypothesised that the mechanical support of the biomaterial scaffold would provide immediate pain relief. Whilst, the delivery of regenerative cells, would provide a long term, gradual regeneration of an ECM which biologically functions, akin to native NP tissue. To date, a variety of biomaterial scaffolds have been investigated for repair of the NP. However injectable scaffolds with the potential to deliver cells, have not demonstrated the required mechanical robustness [14]. Whilst those developed as acellular NP replacement scaffolds have so far failed, due to poor integration resulting in extrusion or expulsion of the implanted material [14,28,29] or are unable to deliver regenerative cells to the IVD [13–16]. The implantation methodology is also an important consideration to minimise trauma to the existing IVD tissue [30,31].

We have previously reported the development of a synthetic Laponite® crosslinked pNIPAM-co-DMAc (L-pNIPAM-co-DMAc) hydrogel delivery system which has the potential to deliver human MSCs (hMSCs) via minimally invasive injection, using small bore needles (26G) which decrease the chance of inducing damage to the annulus fibrosus [23]. We have demonstrated *in vitro* that hMSCs incorporated into L-pNIPAM-co-DMAc hydrogels and cultured in 5% O_2, differentiated into NP-like cells, without the use of chondrogenic inducing medium or additional growth factors [23]. The clinical success of this hydrogel is dependent on: integration with surrounding tissue; the capacity to restore mechanical function; as well as supporting the viability and differentiation of delivered MSCs.

In the present study, we investigated the efficacy of several IVD repair strategies including: hMSCs alone, acellular L-pNIPAM-co-DMAc hydrogel or hMSCs incorporated within L-pNIPAM-co-DMAc hydrogel, injected into bovine NP tissue explants. This study tested the hypothesis that the delivery of hMSCs within the L-pNIPAM-co-DMAc hydrogel would aid scaffold integration, and promote differentiation of MSCs towards the correct NP cell phenotype within native NP tissue. We additionally investigated the mechanical function, defined in this study as disc apparent modulus, strain under load, energy dissipation, and restoration of hydrogel injected bovine IVDs following collagenase digestion. Together these investigations determine the capacity of this hydrogel to be used as both a cell delivery vehicle and as a mechanical support scaffold in the treatment of IVD degeneration.

2. Materials and methods

2.1. Nucleus pulposus tissue explant culture

Bovine tails from 9 months old to 18 months old cows were obtained from the abattoir. Caudal IVDs were excised and NP tissue was isolated. Cores of NP tissue (0.5 cm in diameter) were formed and placed in a Perspex® ring, in sterile 6 well culture plates, as previously described [17]. Ten millilitres of DMEM media (Life Technologies, Paisley UK) supplemented with 10% v/v heat inactivated foetal calf serum (FCS) (Life Technologies, Paisley UK), 100U/ml penicillin (Life Technologies Paisley UK), 100 μg/ml streptomycin (Life Technologies Paisley UK), 250 ng/ml amphotericin (Sigma, Poole UK), 2 mM glutamine (Life Technologies, Paisley UK) and 10 μg/ml ascorbic acid (Sigma, Poole UK) (complete cell culture media) was applied and tissue explants were maintained in culture for 48 h prior to hMSC and hydrogel injection.

2.2. Hydrogel synthesis

An exfoliated suspension of Laponite® clay nanoparticles (25–30 nm diameter, <1 nm thickness) (BYK Additives Ltd, Cheshire UK) was prepared by vigorous stirring of Laponite® (0.1 g) in deionised H_20 (10 ml) (18 MΩ) for 24 h. N-isopropylacrylamide 99% (NIPAM) (0.783 g) (Sigma, Poole UK), N,N′-dimethylacrylamide (DMAc) (0.117 g) (Sigma, Gillingham UK) and 2-2′-azobisisobutyronitrile (AIBN) (0.009 g) (Sigma, Poole UK) were added to the suspension and stirred for 1 h. After passing the suspension through a 5–8 μm pore filter paper, polymerisation was initiated by heating to 80°C and the reagents were allowed to react for 24 h. Following 24 h the hydrogel suspension was cooled to 38–39 °C prior to cell incorporation. Further cooling of the polymeric suspension to 37 °C, i.e. below the lower critical solution temperature (LCST), resulted in rapid gelation to a solidified hydrogel, as previously described [23].

2.3. Mesenchymal stem cell source, expansion and transfer to nucleus pulposus tissue explants

Commercial bone marrow derived human adult mesenchymal stem cells (hMSCs) extracted from a 39 yr old donor (Lonza, Slough UK) were cultured in complete DMEM media (Life Technologies, Paisley UK). MSCs were expanded in monolayer culture to passage 7 to ensure sufficient cells were available. To allow cell tracking following injection, the MSCs were labelled with a fluorescent intracellular carboxyfluorescein N-hydroxysuccinimidyl ester (CFSE) cell labelling kit, (Abcam, Cambridge, UK) according to manufacturer's instructions. Cell seeding solutions were prepared at a density of 4×10^6 cells/ml in either complete DMEM media or liquid hydrogel suspension (38–39 °C) and then 50 μl injected into the centre of NP tissue explants via 26 gauge needle injection (Becton Dickinson, Plymouth, UK). Fifty microliters of media or hydrogel suspension containing no cells was also injected via a 26 gauge needle (Becton Dickinson, Plymouth, UK) into NP tissue explants. This gave four experimental groups: media injected control (control), hMSC injected alone (hMSC), acellular L-pNIPAM-co-DMAc hydrogel (acellular Hy) and hMSC incorporated within L-pNIPAM-co-DMAc hydrogel (hMSC + Hy) injected NP tissue explants. All NP tissue explants were cultured in complete DMEM cell culture media via careful overlay of 10 ml of media per NP tissue explant, incubated at 37 °C, 5% CO_2 and maintained in culture for up to 6 weeks in an oxygen controlled glove box (Coy Lab

products, York, UK) at 5% O_2. Media was replaced every 2–3 days. Samples were removed after 48 h, 2, 4 and 6 weeks for analysis of cell viability, scanning electron microscopy (SEM), histological assessment of matrix deposition and NP cell phenotype analysis using immunohistochemistry (IHC).

2.4. Cytospins

IHC was performed on MSCs taken from monolayer culture prior to injection into NP tissue explants to serve as time zero controls. Monolayer cells were trypsinised and cells fixed in 4% w/v paraformaldehyde/PBS (Sigma, Poole UK) for 20 min, spun at 300 g for 5 min to form a cell pellet and resuspended in PBS to a cell density of 300 cells per microlitre. One hundred microlitres of cell suspension was then cytospun, formed via centrifugation at 1000 rpm for 3 min (Shandon Cytospin 3, Thermo Scientific, Loughborough UK). Slides were subsequently air-dried and stored at 4 °C until required for IHC analysis.

2.5. Processing of tissue explants and identification of the injection site

Triplicate NP tissue explants of each experimental group: control, hMSC alone, acellular Hy and hMSC + Hy, were fixed in 10% w/v formalin (Leica Microsystems, Milton Keynes UK) overnight prior to routine paraffin embedding. Tissue samples were serially sectioned at 4 μm, perpendicular to the needle injection, and two sections every 100 μm were mounted onto positively charged slides (Leica Microsystems, Milton Keynes UK). Sections were air-dried, dewaxed in Sub-X (Leica Microsystems, Milton Keynes UK), dehydrated in industrial methylated spirit (IMS) (Fisher, Loughborough UK), washed in deionised H_2O and then stained with either: routine haematoxylin and eosin (H&E) (Leica Microsystems, Milton Keynes UK); or Hoechst nuclear fluorescent staining (Sigma, Poole UK). Slides stained with H&E were immersed in Mayers haematoxylin for 2 min, rinsed in water for 5 min, immersed in eosin for 2 min, dehydrated in IMS, cleared in Sub-X and mounted in Pertex® (Leica Microsystems, Milton Keynes UK). Slides stained with Hoechst were immersed in 5 pg/mL Hoechst/PBS, incubated for 10 min, washed 3 times in PBS and mounted in 90% v/v glycerol/PBS. Slides were then visualised using light and fluorescent microscopy with an Olympus BX51 microscope and images captured by digital camera and Capture Pro OEM v8.0 software (Media Cybernetics, Buckinghamshire, UK) to identify the injection site and distinguish native NP cells (Hoechst+/CFSE-) and injected hMSCs (Hoechst+/CFSE+). Within control NP explants, the injection site was identified where the needle track could be seen histologically (within early time points) or halfway through the entire depth of the NP tissue explant. Where MSCs were injected alone injection site was determined via the identification of CFSE positive cells. Where acellular L-pNIPAM-co-DMAc or L-pNIPAM-co-DMAc with incorporated MSCs had been injected, the injection site was determined by the histological identification of the hydrogel. Following identification of the position of the injection site and the presence of CFSE positive cells, serial sections in the area of the injection site were mounted onto positively charged slides: for caspase 3 IHC to identify the presence of apoptotic cells, histological assessment of matrix components using Alcian blue and Masson trichrome as well as IHC for aggrecan, chondroitin sulphate and collagen type II to assess phenotypic characteristics.

2.6. Structural and mechanical characterisation

2.6.1. Scanning electron microscopy (SEM)

Samples were removed from culture after 48 h and 6 weeks, frozen at −80 °C and subsequently freeze dried using a FD-1A-50 freeze drier set to −53 °C, 3.8×10^{-4} mbar overnight. The sample was then fractured to expose the interior surface morphology attached onto an aluminium stub and then using a Quorum Technology 150 Q TES system coated with gold (10μA sputter current for 180 s with a 2.7 tooling factor) for imaging.

The fractured surfaces were examined using a FEI NOVA nano-SEM 200 scanning electron microscope (SEM). Secondary electron images were obtained using accelerating voltage 5KV at various magnifications ranging from 1000x to 40,000x.

2.6.2. Hydration degree

To evaluate the hydration degree of NP tissue explants, samples were extracted from culture in triplicate following 48 h, 2, 4 and 6 weeks and the wet weight (M_0) of the NP tissue explants was measured. Samples were then freeze dried using a FD-1A-50 freeze drier set to −53 °C, 3.8×10^{-4} mbar overnight to obtain the dry weight (M_t). The hydration degrees of the NP tissue explants were calculated using Eq. (1):

$$\text{Hydration degree} = \frac{(M_0 - M_t)}{M_0} \times 100 \quad (1)$$

2.6.3. Dynamic mechanical analysis

The mechanical properties of NP tissue explants were characterised following 6 weeks in culture. Replicate samples were removed from culture, blotted and their mechanical properties characterised by DMA. Samples were trimmed using a 5 mm circumference circular biopsy punch from the centre of NP tissue explants, all sample heights were measured and recorded using digital callipers prior to measurement. Triplicate samples were analysed using a PerkinElmer DMA8000 model under confined compression mode at 25 °C, applying a sinusoidal force with a 0.02 mm displacement at 2.5 Hz.

2.7. Histological evaluation of matrix components

Matrix deposition around the injection site of NP tissue explants was investigated following 48 h, 2, 4 and 6 weeks in triplicate. Sections were dewaxed in Sub-X, dehydrated in IMS, washed in deionised H_2O and then stained using histological stains: 1% w/v Alcian blue (pH 2.5) (Sigma Aldrich, Poole UK) in 3% v/v acetic acid (Sigma Aldrich, Poole UK) for 5 min with 1% Neutral red w/v (Sigma Aldrich, Poole UK) used as a counter stain for 2 min or Masson trichrome (Bio-Optica, Miller & Miller (Chemicals) Ltd, Hainault UK) according to the manufacturer's instructions. Sections were dehydrated in IMS, cleared in Sub-X and mounted in Pertex® (Leica Microsystems, Milton Keynes UK). All slides were examined with an Olympus BX51 microscope and images captured by digital camera and Capture Pro OEM v8.0 software (Media Cybernetics, Buckinghamshire, UK). Histological sections were analysed, features noted and images captured to document their histological appearance.

2.8. Immunohistochemistry assessment of apoptosis and phenotypic characteristics

Caspase 3 as a marker of apoptosis and NP matrix markers: aggrecan, collagen type II and chondroitin sulphate were selected for immunohistochemistry (IHC) to assess the viability and phenotypic characteristics of NP tissue explants and delivered hMSCs. IHC was performed as previously described [32]. Briefly, 4 μm paraffin sections were de-waxed, rehydrated and endogenous peroxidase-blocked using hydrogen peroxide (Sigma, Aldrich Poole UK). After washing in tris-buffered saline (TBS; 20 mM tris, 150 mM sodium chloride, pH 7.5) sections were subjected to antigen retrieval methods (Table 1). Following TBS washing, nonspecific binding sites

Table 1
Target antibodies used for IHC, their optimal concentrations and antigen retrieval methods. Heat antigen retrieval consisted of 10-min microwave irradiation in 0.05 M tris buffer, pH 9.5 pre-heated to 60 °C. Enzyme antigen retrieval consisted of 30-min incubation in TBS; 20 mM tris, 150 mM sodium chloride, 46.8 mM calcium chloride dihydrate pH 7.5, containing 0.01% w/v α-chymotrypsin from bovine pancreas at 37 °C.

Target antibody	Clonality	Optimal dilution	Antigen retrieval	Secondary antibody	Serum block
Caspase 3	Rabbit polyclonal	1:400	None	Goat anti rabbit	Goat
Aggrecan	Mouse monoclonal	1:100	Heat	Rabbit anti mouse	Rabbit
Collagen type II	Mouse monoclonal	1:200	Enzyme	Rabbit anti mouse	Rabbit
Chondroitin sulphate	Mouse monoclonal	1:400	Enzyme	Rabbit anti mouse	Rabbit

were blocked at room temperature for 90 min with 25% w/v serum (Abcam, Cambridge, UK) (Table 1) in 1% w/v bovine serum albumin in TBS. Sections were incubated overnight at 4 °C with the appropriate primary antibody (Table 1). Negative controls in which mouse or rabbit IgGs (Abcam Cambridge UK) replaced the primary antibody at an equal protein concentration were used (Table 1). After washing in TBS, sections were incubated in 1:500 biotinylated secondary antibody (Table 1). Disclosure of secondary antibody binding was by the HRP-streptavidin biotin complex (30 min incubation) (Vector Laboratories, Peterborough, UK), TBS washing, followed by application of 0.08% v/v hydrogen peroxide in 0.65 mg/ml 3,3′-diaminobenzidine tetrahydrochloride (Sigma Aldrich, Poole UK) in TBS (20 min incubation). Sections were counterstained with Mayer's haematoxylin, dehydrated in IMS, cleared in Sub-X and mounted in Pertex®. All slides were visualised using an Olympus BX51 microscope and images captured by digital camera and Capture Pro OEM v8.0 software (Media Cybernetics, Buckinghamshire, UK). Evaluation of caspase 3 IHC staining was performed by counting immunopositive and immunonegative cells for each section and immunopositive cells expressed as a percentage of the total count. Images were captured for IHC staining of NP markers: aggrecan, collagen type II and chondroitin sulphate to qualitatively analyse the injection site, native disc cells/injected cells and surrounding matrix.

2.9. Mechanical characterisation of L-pNIPAM-co-DMAc hydrogel injected whole bovine IVDs

2.9.1. IVD isolation and collagenase digestion

Bovine tails from 9 to 18 month old cows were obtained from the abattoir, operating in concordance with animal welfare regulations. Tails were stored at −20 °C shortly post sacrifice and tested a maximum of one month post storage. Tails were thawed at 5 °C for 24 h prior to sample preparation. Discs were dissected whole from tail sections between cd1-2 and cd4-5. Discs without parallel faces or with visible signs of damage were discarded. The remaining discs were allowed to equilibrate to room temperature for 12 h before testing, between 2 and 4 discs were gained from each tail section. Discs were stored in airtight sealed bags to prevent dehydration during this time. Discs were randomly assigned to four test groups (n = 10 per group): healthy; sham injected; collagenase digested and collagenase digested following hydrogel injected. Healthy discs were not experimentally manipulated following excision, sham injected discs were stabbed with a 21-gauge needle to assess the effect of needle insertion. Collagenase digested and hydrogel injected discs were injected with 100–200 μl of a 2 mg/mL collagenase solution (Sigma, Poole, UK) in distilled water (injection was performed until either the internal pressure in the disc prevented any further injection or a maximum of 200 μl had been injected) and incubated for 2 h at 37 °C.

2.9.2. Injection of L-pNIPAM-co-DMAc hydrogel in whole bovine IVDs

Following collagenase digestion, discs to be injected with hydrogel were inspected morphologically to ensure collagenase digestion had successfully induced void formation. Hydrogel injected discs then received an injection of 50–200 μL of acellular L-pNIPAM-co-DMAc hydrogel, with an incorporated green food dye for visulisation. Hydrogel injected discs were left 30 min post injection to allow the L-pNIPAM-co-DMAc hydrogel to stabilize and mimic the operation time for the patient, prior to testing. Injection protocol consisted of the syringe being depressed until either the internal pressure in the disc prevented any further intake or a maximum of 200 μl of L-pNIPAM-co-DMAc hydrogel had been injected. All the needle tips were inserted into the centre of the NP before injection of material. Visual inspection during injection allowed needle position to be observed through the deformation of surrounding material.

2.9.3. Mechanical loading of IVDs

Discs were loaded cyclically using a dynamic test rig incorporating a hydraulic piston controlled by Wavematrix 1.8 test software and a Labtronic 8800 hydraulic controller (Instron. Mass, USA). Discs were placed between two smooth parallel metal platens without further constraint. Discs with non-parallel surfaces were rejected prior to testing and no lateral movement was observed during testing (indicating that disc surfaces were parallel and all deflection was in the axial direction). Discs were subjected to a sinusoidal load between 0.53 and 0.65 MPa at 2 Hz to simulate walking based on known values from the literature [51–53]. Each disc was ramped to a preload at the midpoint between the upper and lower boundaries at a rate of 0.01 kN/s, immediately upon reaching the preload, cyclic loading was applied for 100 s, representative of a short period of activity typical of activities of daily living (ADLs) in all but the most severely impaired persons.

Three measures of mechanical response were tracked by the data acquisition tools connected to Wavematrix. Engineering stiffness of each disc was measured as the change in force divided by the change in displacement from minimum (Fmin = 0.53 MPa × disc cross-sectional area) to maximum (Fmax = 0.65 MPa × disc cross-sectional area) loading. Strain was measured as the displacement between those points divided by the disc height at minimum loading. Lastly the energy dissipated by discs during each loading/unloading cycle was calculated from the hysteresis in the load deflection data and converted to J/cycle.

2.10. Data processing and statistical analysis

All tests were performed at least in triplicate. Data was assessed for normality using the Shapiro Wilks test and found to be non-parametric and hence statistical comparisons were performed by Kruskal-Wallis with a pairwise comparisons (Conover-Inman) post hoc test performed with statistical significance accepted at $p \leq 0.05$. Pairwise comparisons were made as follows: between all-time points and between the different experimental groups for caspase 3 immunopositivity; between the different experimental groups for mechanical analysis; hMSC alone, Acellular Hy and hMSC + Hy compared with media injected control NP explants for hydration assessment at each given time point. Data was then presented on graphs; all replicates have been shown with median value indicated to demonstrate clearly the spread of replicates.

3. Results

3.1. Identification of injected L-pNIPAM-co-DMAc hydrogel and mesenchymal stem cells

No CFSE (green) positive cells were identified within media injected controls or acellular hydrogel injected NP tissue explants (Fig. 1). CFSE positive MSCs were identified where MSCs had been injected alone, where they remained in clusters at the vicinity of the injection site following 4 weeks in culture (Fig. 1). Some CFSE positive cells appeared to have migrated away from the injection site following 6 weeks, although many were still in close proximity to each other (Fig. 1). Infiltrating native NP cells stained with Hoechst were identified within the acellular L-pNIPAM-co-DMAc following 4 and 6 weeks in culture (Fig. 1). CFSE positive MSCs were identified within the L-pNIPAM-co-DMAc hydrogel throughout the 6 week culture duration where they had been incorporated prior to injection (Fig. 1). CFSE positive MSCs were also observed within the native NP tissue surrounding the hydrogel region following 6 weeks in culture (Fig. 1).

3.2. Caspase 3 cell viability

Low levels of apoptosis was observed in media injected control NP explant tissue, with no significant difference in the number of caspase 3 immunopositive cells throughout the 6 week culture duration (Fig. 2a, b). Where acellular L-pNIPAM-co-DMAc hydrogel had been injected no significant difference in the number of caspase 3 immunopositive cells was observed between native NP cells within the surrounding NP tissue compared with native NP cells infiltrated within the hydrogel (Fig. 2a, b). Low levels of apoptosis within MSCs injected alone, with no significant difference in the number of immunopositive cells observed throughout the 6 week culture duration (Fig. 2a, b). Where MSCs were incorporated within L-pNIPAM-co-DMAc hydrogel prior to injection, no significant difference in the number of caspase 3 immunopositive cells was observed between cells found within the surrounding native NP tissue and cells found within the L-pNIPAM-co-DMAc hydrogel itself (Fig. 2a, b). No significant difference in the number of capsase 3 immunopositive cells was observed between the different experimental groups at any time point (Fig. 2a, b) ($P > 0.05$).

3.3. Structural and mechanical characterisation

3.3.1. Scanning electron microscopy

The interior micro scale morphology of NP tissue explants was examined using scanning electron microscopy (SEM) (Fig. 3). Native NP cells were visualised embedded within a disorganised fibrous collagen matrix, throughout the 6 week culture duration in media injected control explants (Fig. 3). Where MSCs were injected alone clustered cells could be seen following 48 h which appeared to have migrated following 6 weeks in culture (Fig. 3). Injected acellular L-pNIPAM-co-DMAc hydrogel displayed a comparatively uniform interconnecting porous network encapsulated by the surrounding NP tissue following 6 weeks in culture. Where MSCs were incorporated within the L-pNIPAM-co-DMAc hydrogel prior to injection, cells could be seen within the centre of the hydrogel region (Fig. 3); a distinction in the microscale morphology of the interior hydrogel was still evident in comparison to the native surrounding NP tissue following 6 weeks, however integration could be seen at the hydrogel/NP tissue interface with connecting NP tissue fibres penetrating within the outside edges of the hydrogel region (Fig. 3).

3.3.2. Dynamic mechanical analysis

MSC injected and hydrogel injected NP tissue explants displayed similar mechanical properties to media injected control explants with no significant difference in the elastic modulus (G') loss modulus (G'') or tan delta ($\tan\delta$) for any of the experimental groups following 6 weeks in culture (Fig. 4a, b, c).

3.3.3. Hydration assessment

The injection of MSCs alone did not significantly alter the hydration degree of NP tissue explants following 48 h, 4 and 6 weeks in culture, although a significant increase ($P = 0.0011$) in the hydration of hMSC injected alone NP tissue explants was observed in comparison to media injected control explants following 2 weeks in culture (Fig. 4d). Where acellular L-pNIPAM-co-DMAc hydrogel was injected a significant increase ($P = 0.0064$) in the hydration degree was observed in comparison to media injected control explants following 6 weeks in culture (Fig. 4d). Where hMSCs were incorporated into L-pNIPAM-co-DMAc hydrogel prior to injection a significant increase in the hydration degree was observed in comparison to media injected control explants following 2 ($P = 0.0015$) and 6 ($P = 0.0095$) weeks in culture in comparison to control explants (Fig. 4d).

3.4. Histological evaluation of matrix components

Reduced matrix staining for both proteoglycans, and collagen was observed throughout the 6 week culture period within media injected control NP explants (Fig. 5). Where MSCs were injected alone, blue staining for proteoglycans was present within and surrounding the cell clusters, although the staining intensity was less than that of the native surrounding NP tissue (Fig. 5). Areas of blue staining for collagen were also observed within cell clusters where MSCs had been injected alone, although the majority of cells present within the clusters were negative (red) for collagen staining (Fig. 5). Positive blue matrix staining for both proteoglycans and collagen was observed within the acellular L-pNIPAM-co-DMAc hydrogel which had been injected into NP explants, particularly following 4 and 6 weeks (Fig. 5). A distinct native NP tissue border, with high intensity collagen staining, was observed surrounding the acellular L-pNIPAM-co-DMAc hydrogel following 48 h, 2 and 4 weeks in culture (Fig. 5). Blue positive proteoglycan and collagen producing cells were observed within the L-pNIPAM-co-DMAc hydrogel where hMSCs had been incorporated prior to injection throughout the 6 week culture duration (Fig. 3). Native NP tissue directly adjacent to L-pNIPAM-co-DMAc hydrogel with incorporated hMSCs, demonstrated strong intensity staining for both proteoglycans and collagen (Fig. 5). A distinct NP tissue border, with high intensity collagen staining, was present surrounding the L-pNIPAM-co-DMAc hydrogel, where MSCs were incorporated, following 48 h and 2 weeks in culture, however this was subsequently absent with integration of the surrounding NP tissue within the hydrogel observed following 4 and 6 weeks in culture (Fig. 5).

3.5. Immunohistochemical evaluation of cell phenotype

Immunohistochemistry was used to assess the expression and localisation of the NP matrix markers collagen type II, aggrecan and chondroitin sulphate within MSCs, both in monolayer and following injection into NP tissue explants, as well as within native NP cells within the explant tissue (Fig. 6). Collagen type II, aggrecan and chondroitin sulphate was expressed by all native NP cells found with control, acellular L-pNIPAM-co-DMAC injected, hMSC only injected and hMSC incorporated within L-pNIPAM-co-DMAc injected NP tissue explants, throughout the 6 week culture duration (Fig. 6). Immunopositive cells for collagen type II, aggrecan and chondroitin sulphate were identified surrounding the acelllular L-

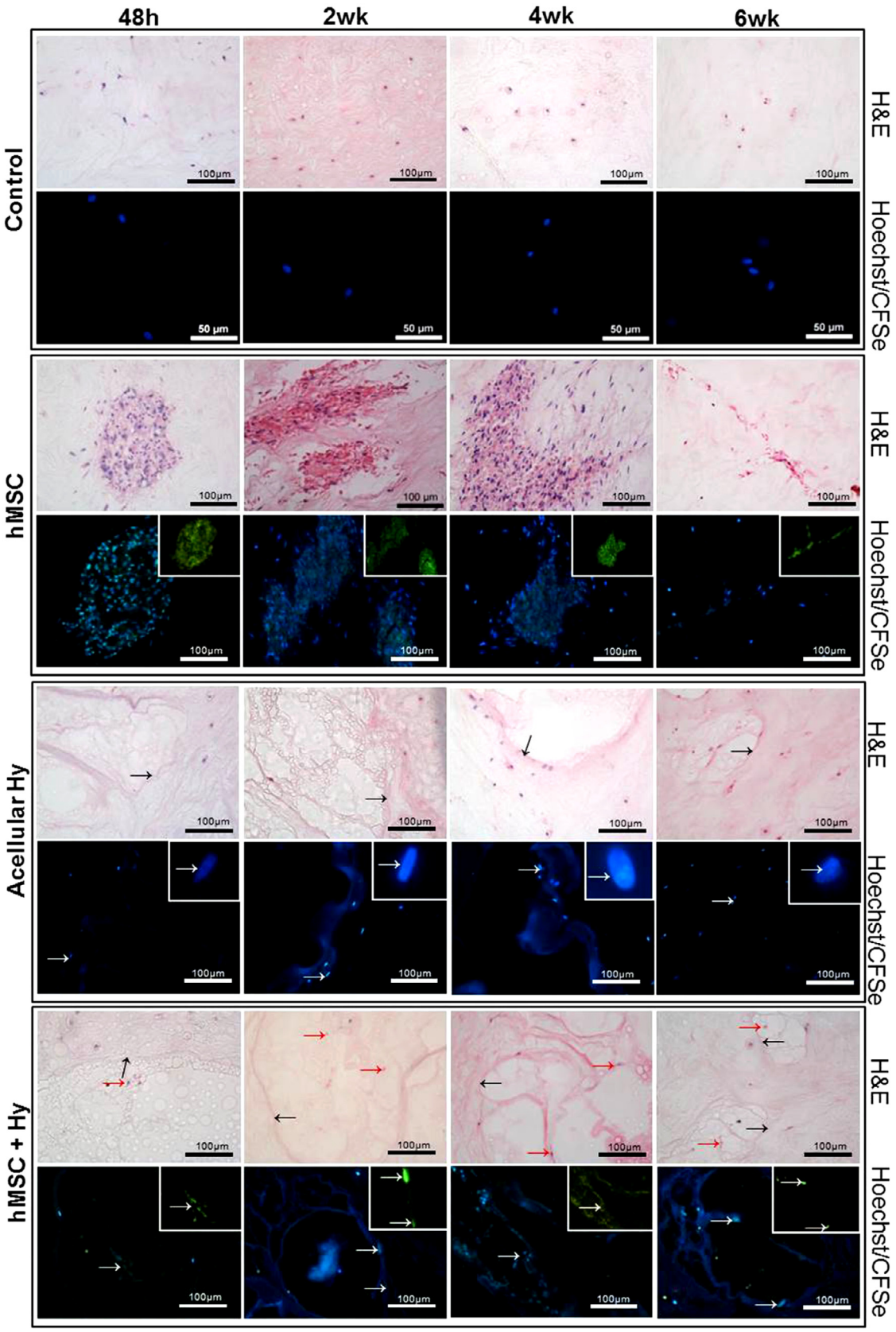

Fig. 1. Photomicrographs of haematoxylin & eosin stain, Hoechst staining and green fluorescent protein CFSE positive cells (shown inset for hMSC and hMSC + Hy NP tissue explants) in the injection sites of bovine nucleus pulposus tissue following 48 h, 2, 4 and 6 weeks in culture. Magnified images of native NP cells, stained with Hoechst, surrounding acellular hydrogel, shown inset to aid visualisation. White arrows on acellular Hy images indicate cells, black arrows on H&E images indicate hydrogel/tissue interface, red arrows on H&E images for hMSC + Hy indicate cells within hydrogel. Media injected control tissue (Control), CFSE positive hMSC injected alone (Injected hMSC), L-pNIPAM-co-DMAc hydrogel injected without cells (Acellular Hy) and hMSC incorporated into L-pNIPAM-co-DMAc hydrogel injected (hMSC + Hy). Scale bar = 50 µm or 100 µm. (For interpretation of the references to colour in this figure legend, the reader is referred to the web version of this article.)

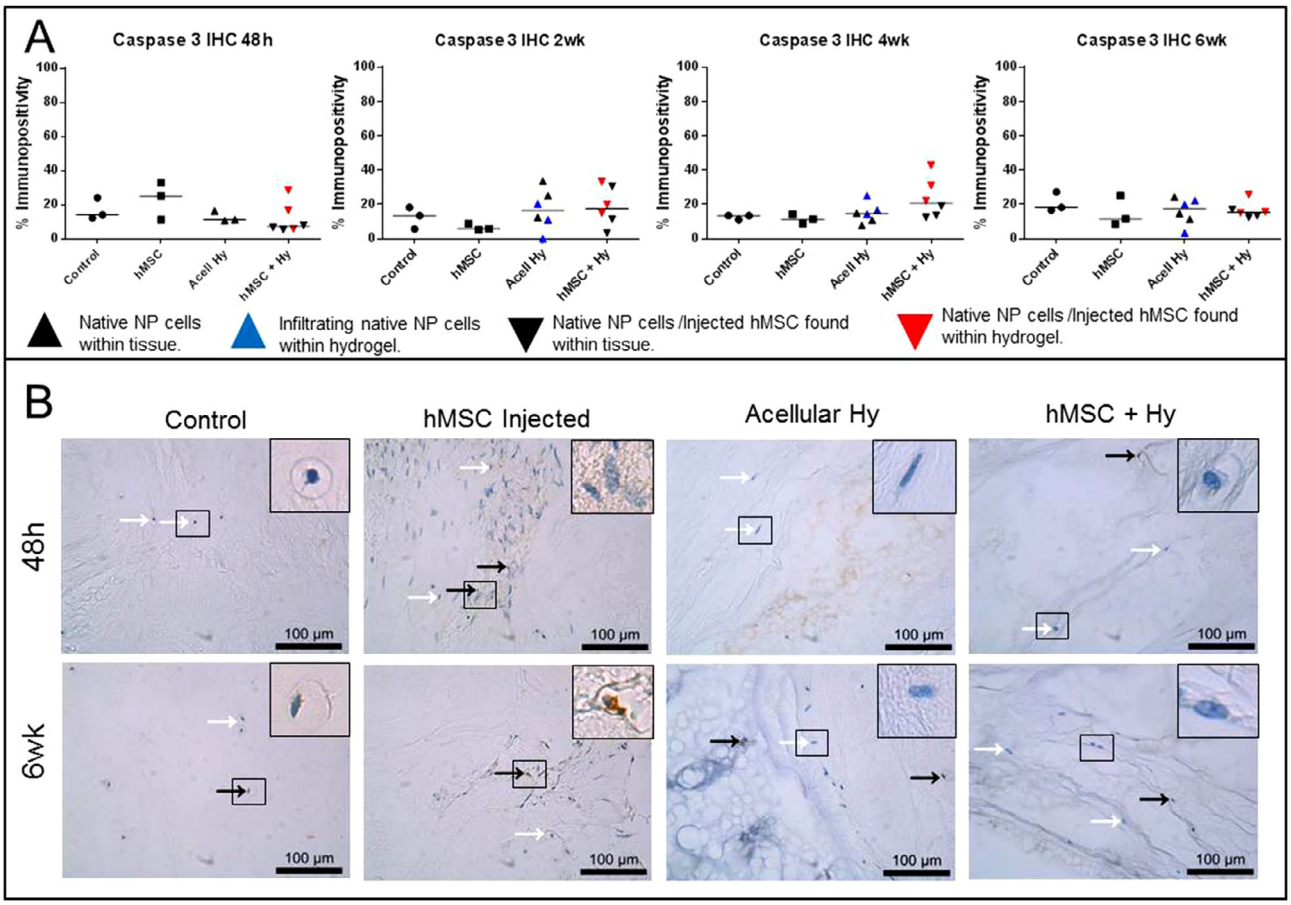

Fig. 2. Immunohistochemical detection of caspase 3 to assess cell viability after 48 h, 2, 4 and 6 weeks in culture. Percentage immunopositivity was calculated (A). Photomicrographs representative of caspase 3 immunopositivity in tissue explants at 48 h and 6 weeks post injection (B). Back arrows indicate positively stained cells and white arrows indicate negatively stained cells. Scale bar = 100 µm.

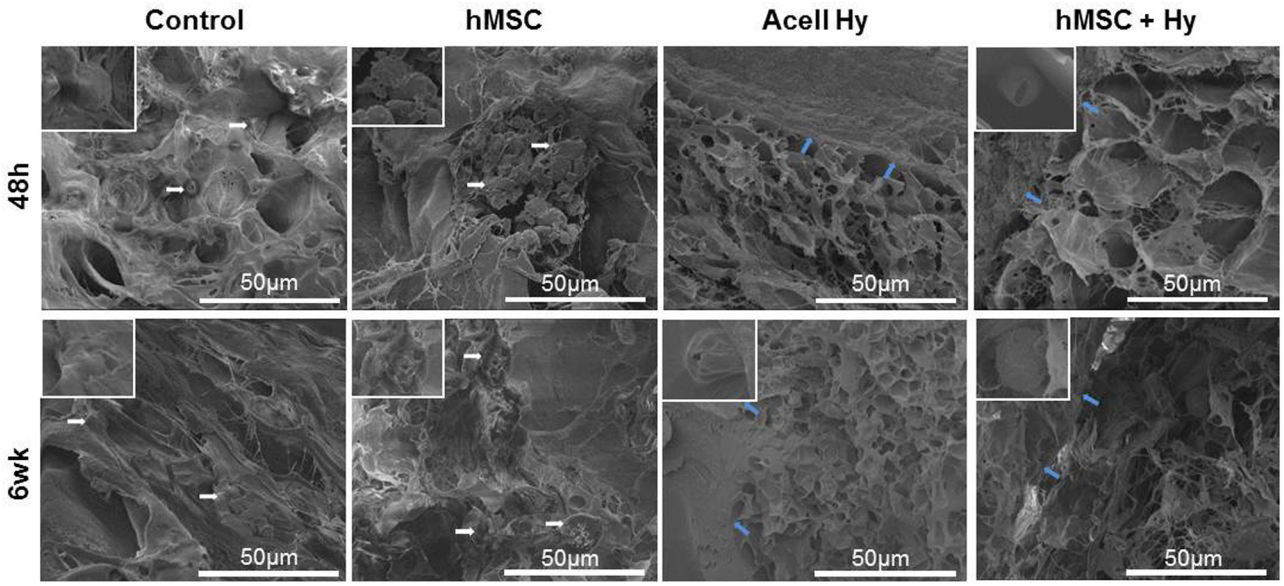

Fig. 3. Scanning Electron Microscopy (SEM) of media injected control (Control), hMSC injected alone (hMSC), Acellular L-pNIPAM-co-DMAc hydrogel injected (Acellular Hy) and hMSC incorporated within L-pNIPAM-co-DMAC hydrogel injected (hMSC + Hy) NP tissue explants following 48 h and 6 weeks in culture. Enlarged images of native NP cells (control), hMSCs (hMSCs injected alone) and cells within hydrogel region (Acell 6 weeks, hMSC + Hy 48 h and 6 weeks) shown inset for visualisation. White arrows indicate native NP cells within Control NP explants and presence of hMSCs within hMSC injected alone NP explants. Blue arrows indicate NP tissue/hydrogel interface, demonstrating integration of hydrogel with surrounding NP tissue. Scale bar 50 µm.

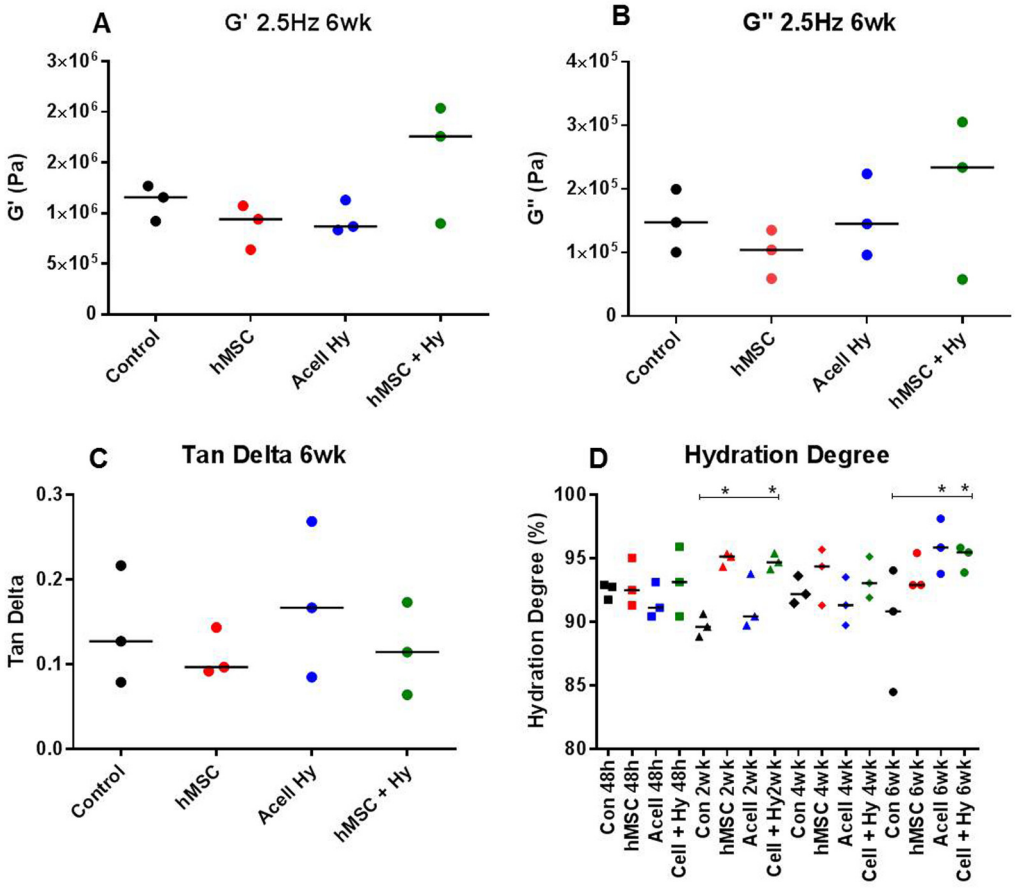

Fig. 4. Mechanical analysis of bovine explant NP tissue using dynamic mechanical analysis (A, B, C). (A) Elastic modulus (G′), (B) loss modulus (G″) and (C) Tan Delta (tanδ) at 2.5 Hz after 6 weeks in culture. (D) Calculated hydration degree of bovine explant tissue throughout 6 weeks in culture. Media injected control (con), hMSC injected alone (hMSC), acellular L-pNIPAM-co-DMAc injected (Acell Hy) and hMSC incorporated into L-pNIPAM-co-DMAc injected (hMSC + Hy). (*) Indicates statistical significance compared to controls at each timepoint (D) ($^{*}p = \leq 0.05$).

pNIPAM-co-DMAc hydrogel following 48 h, 2 and 4 weeks in culture, with some immunopositive native NP cells for collagen type II, aggrecan and chondroitin sulphate observed within the acellular L-pNIPAM-co-DMAc hydrogel following 6 weeks in culture (Fig. 6). Monolayer MSCs extracted from culture prior to injection into NP tissue explants showed no immunopositivity for aggrecan, with low levels of immunopositivity for chondroitin sulphate (average 52% range 50–55%) and collagen type II (average 17% range 14–20%) (Suppl Fig. 1). Immunopositive cellular and matrix staining for collagen type II, aggrecan and chondroitin sulphate was observed within the vicinity of the cell clusters where hMSCs had been injected alone, from 48 h to 6 weeks in culture (Fig. 6). Intense matrix staining and positive cellular staining for collagen type II, aggrecan and chondroitin sulphate was observed within the L-pNIPAM-co-DMAc hydrogel where MSCs had been incorporated prior to injection (Fig. 6). NP tissue with high intensity matrix staining for collagen type II and chondroitin sulphate was present integrating within the L-pNIPAM-co-DMAc hydrogel where MSCs had been incorporated prior to injection, following 6 weeks in culture (Fig. 6). All IgG control sections for collagen type II, aggrecan and chondroitin sulphate showed no immunopositivity (suppl Fig. 1).

3.6. Mechanical characterisation of L-pNIPAM-co-DMAc hydrogel injected whole bovine IVD

Whole bovine IVDs subjected to loading simulating a short period of walking demonstrated a different mechanical response depending on the treatment regime of the disc. When differences in disc size were accounted for and outliers excluded healthy discs had 1.88 times higher stiffness (24.3–12.9 MPa) (Fig. 7A), 80% lower strain (0.54–2.7%) (Fig. 7B) and 2.8 times greater energy dissipation (2.12–0.76 J/cycle) (Fig. 7C) compared to discs that had undergone collagenase digestion, with $P < 0.001$ in each case when outliers were accounted for (Fig. 7). Discs subjected to collagenase digestion could be seen in 6 out of 10 discs to display clear digestion of the IVD (Fig. 7) with alteration to mechanical properties, however 4 discs which were injected with collagenase failed to show evidence of digestion (no voids visible) and thus were removed from the statistical analysis and showed as red outliers (Fig. 7). Discs subjected to the same collagenase treatment process following observation of clear evidence of digestion morphologically were subsequently injected with L-pNIPAM-co-DMAc hydrogel, these discs demonstrated a complete recovery of disc stiffness, displaying only non-significant ($P > 0.05$) differences from healthy disc stiffness (24.3–26.4 MPa) (Fig. 7A) and strain values (0.54–0.5%) (Fig. 7B). However there was no recovery of the discs ability to dissipate energy (Fig.7C), with hydrogel injected discs dissipating less energy than any other test group (0.40 J/cycle), significantly ($P < 0.001$) lower than even collagenase digested discs (Fig. 7c). Discs injected with hydrogel containing green dye could be clearly identified macroscopically (Fig. 7D, E) and microscopically were shown to fill the fissures formed via collagenase digestion (Fig. 7F, G).

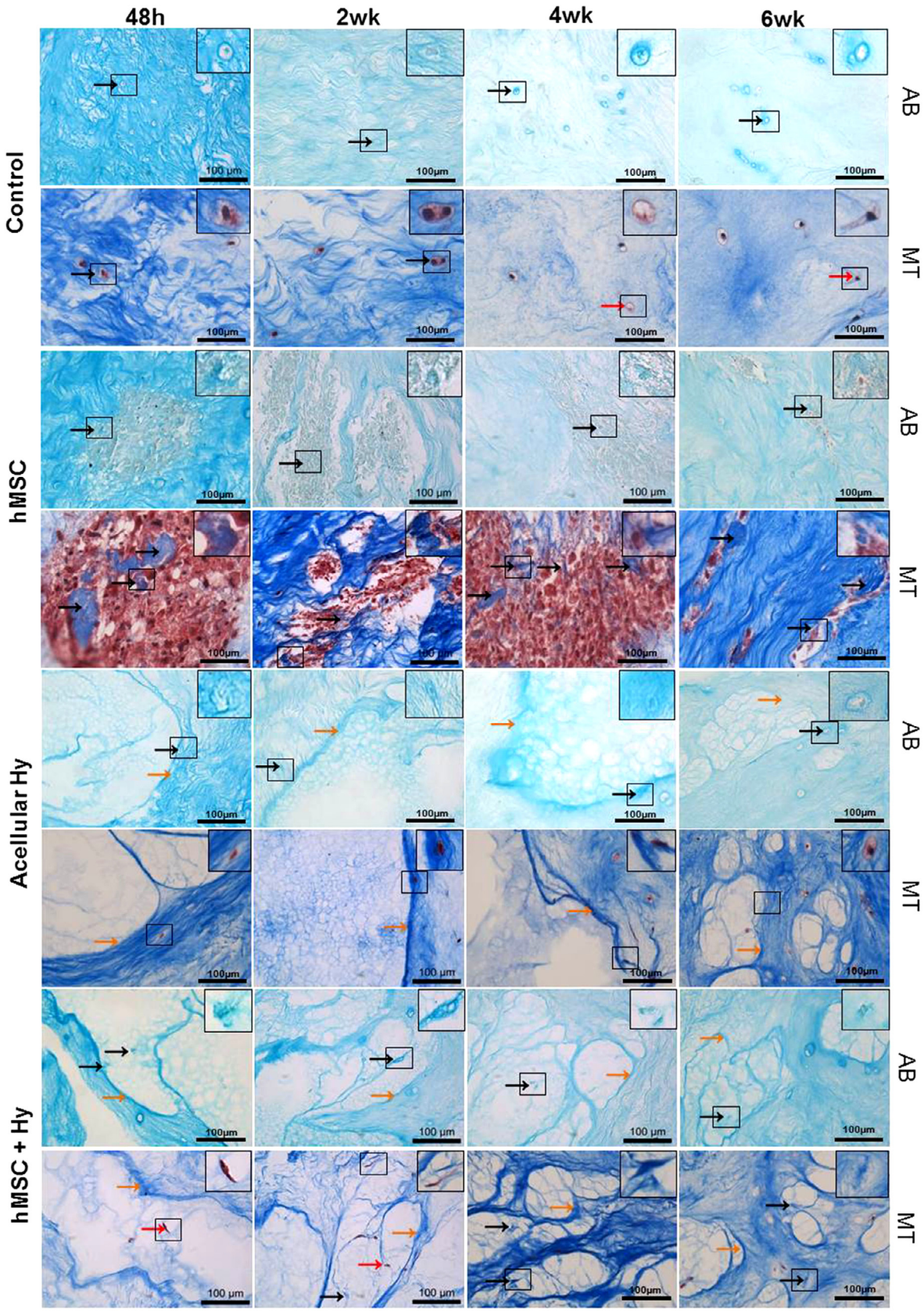

Fig. 5. Histological evaluation of bovine NP tissue explants using Alcian blue (AB) for proteoglycan deposition and Masson trichrome (MT) for collagen deposition after 48 h, 2, 4 and 6 weeks in culture. Media injected control tissue (control), hMSCs injected alone (hMSC), Acellular L-pNIPAM-co-DMAc injected (Acellular Hy) and hMSCs incorporated within L-pNIPAM-co-DMAc hydrogel injected (hMSC + Hy). Black arrows indicate positively stained cells, red arrows indicate negatively stained cells and orange arrows indicate hydrogel/NP tissue interface. Magnified images of representative cells shown inset for visualisation. Scale bar = 100 µm.

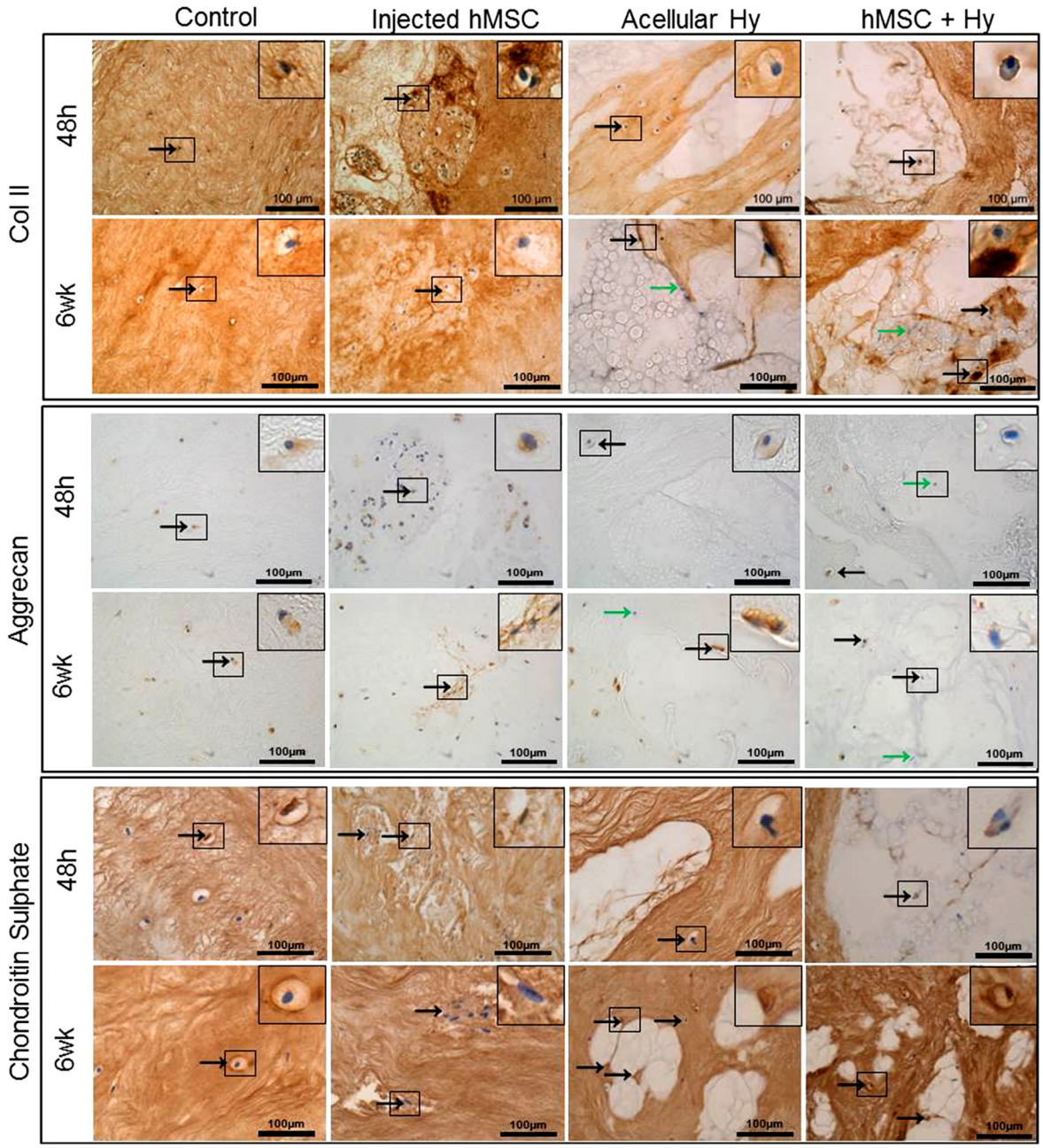

Fig. 6. Immunohistochemical detection of NP matrix markers collagen type II, aggrecan and chondroitin sulphate in bovine NP tissue explants. Representative photomicrographs after 48 h, and 6 weeks in culture. Black arrows demonstrate positively stained cells and green arrows demonstrate negatively stained cells. Enlarged immunopositive cells shown inset for visualisation. Scale bar = 100 µm. (For interpretation of the references to colour in this figure legend, the reader is referred to the web version of this article.)

4. Discussion

4.1. Evaluation of biological performance to act as a cell delivery vehicle

The clinical translation of hydrogels specifically developed for the delivery of regenerative cells to the IVD is dependent on several requirements: that they can be administered by a minimally invasive procedure that delivers the required cell population without detrimental effects to both the implanted cells and surrounding tissues during delivery. That they are biocompatible and thus support the viability of delivered cells and native cell populations. The hydrogel should facilitate cellular migration to aid in the integration with surrounding tissue to prevent biomaterial extrusion. Finally, the hydrogel can support and promote the differentiation of delivered MSCs into biologically functional NP like cells in order to repair and regenerate a matrix akin to native NP tissue.

4.1.1. Minimally invasive delivery of L-pNIPAM-co-DMAC hydrogel

In our previous *in vitro* studies we have demonstrated that hMSC could be incorporated into liquid L-pNIPAM-co-DMAc hydrogel, injected through a narrow 26-gauge needle before solidification at 37 °C with no detriment to cell viability [23,33]. Here, acellular L-pNIPAM-co-DMAc hydrogel was injected through the AF into collagenase digested bovine IVD via 26-gauge needle injection. The hydrogel was maintained within the disc during

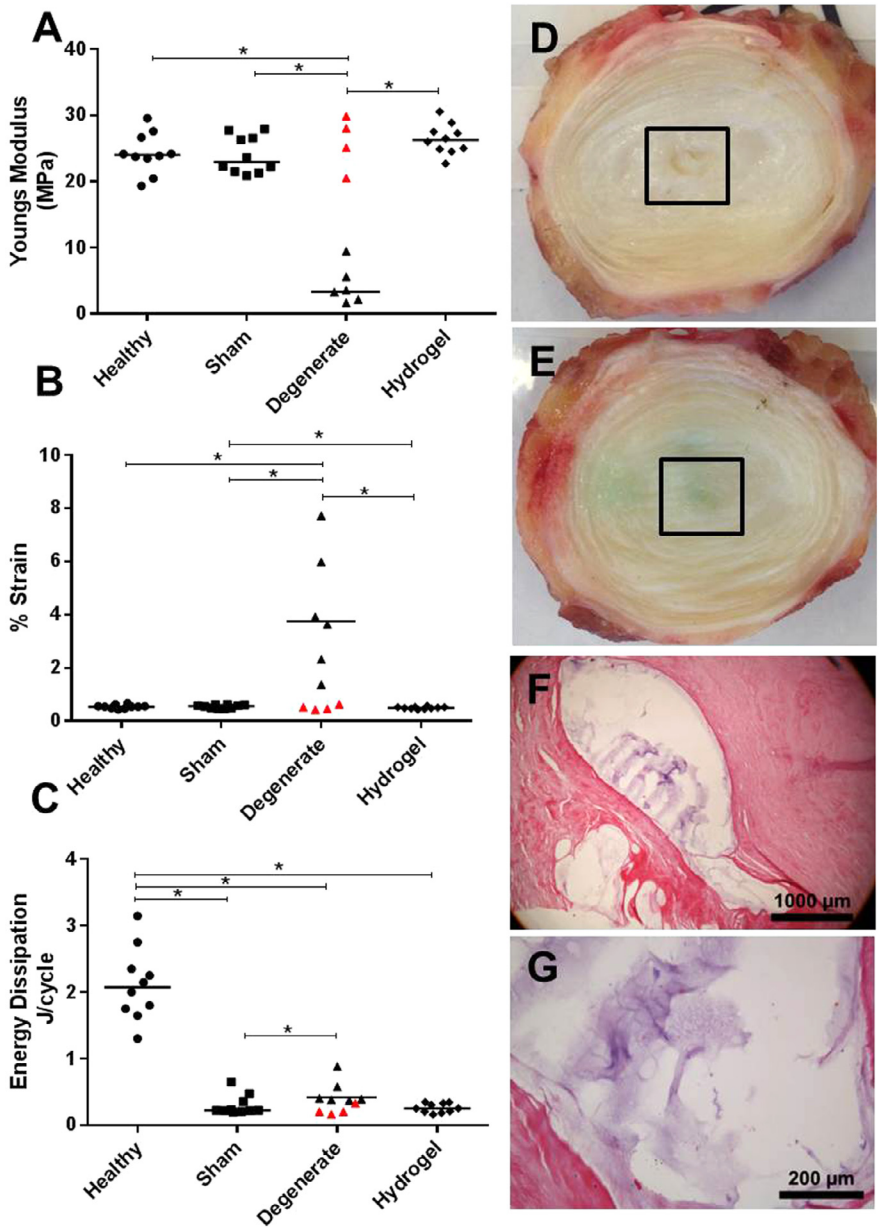

Fig. 7. Mechanical analysis of whole bovine IVDs that were healthy, stabbed with 21 G needle (sham), collagenase digested or collagenase digested followed by hydrogel injection (hydrogel). Measured parameters include: (A) Young's Modulus, (B) % Strain and (C) Energy Dissipation. Four discs (red) from the digested group demonstrated young's modulus and strain behaviour similar to sham injected suggesting collagenase injection had been insufficient and this was supported by the lack of morphological evidence of collagenase digestion in these discs, thus were marked as outliers but energy dissipation was in line with other needle punctured discs. All replicates have been shown with outliers marked in red to demonstrate clearly the spread of replicates. Median values indicated do not include outliers within digested group. (*) Indicates significant differences between experimental groups ($p = \leq 0.05$). (D) Representative macroscopic image of whole bovine IVD following collagenase digestion (average IVD diameter 30 mm). (E) Representative macroscopic image following collagenase digestion and hydrogel injection, with a green food dye incorporated within the hydrogel to aid visualisation. (F, G) Microscopic images stained with haematoxylin and eosin of whole IVD following collagenase digestion, hydrogel injection and mechanical loading. Scale bar 1000 μm, 200 μm. (For interpretation of the references to colour in this figure legend, the reader is referred to the web version of this article.)

mechanical loading and shown histologically to infiltrate micro and macro fissures akin to those which could occur during IVD degeneration. The selected needle diameter is an important design consideration which is often dictated by the viscosity of the biomaterial being injected [34]. It is generally accepted that the needle diameter should be as narrow as possible to avoid structural and mechanical damage to surrounding tissues during injection. However decreasing the needle diameter for viscous biomaterials increases injection pressures which can increase shear forces on cells reducing cell viability [34,35]. The low viscosity (0.97 MPas at 54 °C) [23] of the L-pNIPAM-co-DMAC liquid hydrogel, enabled its injection with incorporated hMSCs into NP tissue explants with no loss in viability. The minimally invasive route demonstrated here offers significant advantage over previously developed hydrogels implanted into IVD tissue where nucleotomy was required to create a void for the biomaterial to occupy [13–16,36], or large diameter surgical implanting tools were used [37]. Moreover, the synthetic route utilised, which exploits the thermal phase transi-

tion of a fully reacted polymer in the liquid state, offers rapid solidification at 37 °C. This maintains the L-pNIPAM-co-DMAC hydrogel and incorporated hMSCs within the injection site, whilst avoiding the need for additional implantation devices to initiate *in situ* polymerisation such as those proposed for photopolymerised hydrogels [15,25,34].

4.1.2. Biocompatibility of L-pNIPAM-co-DMAc hydrogel

The biocompatibility of delivered hMSCs is essential if the repopulation of cells for the long term recovery and regeneration of a functional NP matrix is to be a viable therapeutic option in the treatment of IVD degeneration. In agreement with previous studies [17,20,38–42], excellent viability across all time points and all treatment regimes were observed. However, despite mimicking the hypoxic disc microenvironment, it should be noted that the culture conditions used in this study do not completely reflect that of the native IVD in terms of a mechanically loaded environment [43] and low nutrient supply [44]. Moreover, the degenerate IVD is an extremely hostile biological environment with increased production of matrix degrading enzymes [6] and pro-inflammatory cytokines [8,9] which may affect viability *in vivo*. Future investigations to ascertain the survival of delivered MSCs within such conditions is paramount to the clinical translation of this kind of therapy. However the survival of MSCs incorporated within the L-pNIPAM-co-DMAc hydrogel, is extremely promising since the use of the hydrogel as a delivery system also provides the opportunity to simultaneously deliver antagonists of catabolic mediators if required.

4.1.3. Integration of L-pNIPAM-co-DMAc hydrogel

The infiltration of native NP cells, demonstrated in both acellular and hMSC incorporated within the L-pNIPAM-co-DMAc hydrogel injected into NP explants, is particularly important to aid in scaffold integration with the surrounding NP tissue. Restoring optimum mechanical function and prevent issues such as biomaterial extrusion [14,45]. Integration of L-pNIPAM-co-DMAC hydrogel with surrounding NP tissue was particularly evident in this study, with deposited matrix penetrating within the hydrogel/tissue interface shown histologically and using SEM. Despite initial fibrous encapsulation observed surrounding the hydrogel following 4 weeks in acellular L-pNIPAM-co-DMAc hydrogel injected NP tissue explants, it is hypothesised that dynamic culture under mechanical load would promote and accelerate the hydrogel tissue integration, as dynamic compressive mechanical loading has been shown to promote NP matrix biosynthesis [46], increase NP cell metabolism [46,47] and promote proliferation and differentiation of MSCs into NP-like cells [48,49].

4.1.4. Differentiation of MSCs following injection into NP tissue explants

In agreement with previous studies [17], where MSCs were injected alone into NP tissue explants, the cells were maintained within clusters at the vicinity of the injection site for up to 4 weeks, although migration was evident following 6 weeks in culture. Migration and differentiation of these cells into NP like cells is essential for efficacious NP matrix repair. Here MSCs injected alone were shown to produce NP matrix components collagen type II, aggrecan and chondroitin sulphate. The deposition of this matrix was localised immunohistochemically to the clusters of MSCs visualised, indicating that the MSCs themselves were responsible for the matrix synthesis; this is in agreement with previous studies [17,20,39]. Despite this, a major concern for the clinical translation of stem cell therapy for the treatment of IVD degeneration is a lack of control over the differentiation capacity of these cells following injection into nucleus pulposus tissue [27]. In addition, the location of these cells following injection is crucial since MSC leakage followed by undesirable bone formation has been reported previously as a potential side effect of this therapeutic strategy [26]. The incorporation of MSCs within the L-pNIPAM-co-DMAc hydrogel during the liquid phase for delivery, is advantageous as it ensures the interconnecting porous hydrogel network is able to assemble around the cells. This ensures that in the initial weeks following injection, the cells are maintained within the injection site and that the microenvironment of the hydrogel itself will be the first structural influence on the differentiation capacity of the MSCs. This gives a greater potential control over the differentiation and location of the delivered regenerative cells. We have previously demonstrated *in vitro* that MSCs incorporated into L-pNIPAM-co-DMAc hydrogel and cultured under hypoxic conditions induces differentiation of MSCs into NP like cells without the need for additional chondrogenic inducing medium or growth factors [23]. Here, we have shown that cells incorporated into L-pNIPAM-co-DMAc hydrogel and injected into NP explants were shown to produce NP matrix components: collagen type II; aggrecan and chondroitin sulphate. We are unable to ascertain whether the matrix deposition itself is from the delivered MSCs or native NP cells, it is most likely to be a combination of both since positive cells and deposited matrix which compositionally reflects native NP tissue, was observed both within the hydrogel itself and surrounding the hydrogel/tissue interface. Thus the translation of our previous *in vitro* results within an *ex vivo* NP tissue explant model demonstrated here, offers significant promise for the efficacy of this therapeutic strategy in the delivery of MSCs for the repair and regeneration of the NP as a future treatment of IVD degeneration. A short coming of the current study is that commercial MSCs were utilised, thus future investigations should be conducted to assess the differentiation of MSCs from a large cohort of human patients to determine patient variability and age of patients which can be utilised for such a therapy.

4.2. Evaluation of mechanical properties to act as a support scaffold

The NP is regarded as a viscoelastic material, exhibiting both fluid and solid like behaviours [50]. It has been well documented that the viscoelasticity of NP tissue changes with ageing and degeneration, exhibiting a more ‘solid-like’ than ‘fluid-like’ behaviour, reflected by a decreased tanδ [51]. One of the hallmarks of IVD degeneration is a reduction in the overall proteoglycan content [7] resulting in reduced tissue hydration [4,52,53]. The injection of a hydrogel biomaterial, defined as a 3D hydrated crosslinked polymeric network, has therefore been hypothesised as an appealing strategy to restore NP tissue hydration and thus potentially regain some of the viscoelastic NP material properties [54,55]. The significant increase in hydration degree of NP tissue explants following 6 weeks where acellular and hMSC incorporated L-pNIPAM-co-DMAc hydrogel was injected, provides promising evidence to suggest that the L-pNIPAM-co-DMAc hydrogel material itself is compositionally advantageous to the overall NP tissue hydration. The benefits of which would be even more apparent within degenerate tissue. Despite the increased hydration degree no significant difference in the G′, G″ or the tanδ were observed regardless of whether hMSCs or L-pNIPAM-co-DMAc hydrogel were injected. This is likely due to the fact that the NP tissue explant controls used in this study were not experimentally manipulated to be degenerate; thus the fact that there is no statistical difference in the viscoelastic parameters assessed between the different experimental groups, indicates that both hMSC and L-pNIPAM-co-DMAc hydrogel injected NP tissue explants display similar biomechanical properties to native NP tissue. A limitation that should be considered however is that in this study the NP tissue explants were statically cultured within a semi-constrained Perspex ring culture system, therefore the biomechanical proper-

ties of the explant NP tissue is likely to be different from native NP tissue found within the body [49,56].

Loading of whole bovine collagenase digested IVDs injected with L-pNIPAM-co-DMAc hydrogel, demonstrated a significant recovery of structural properties, completely regaining pre-digested levels of disc stiffness. The full recovery of disc mechanical response following hydrogel injection, shown in this study, is a highly promising result, providing supporting evidence that the hydrogel could offer a significant and near immediate structural benefit to degenerate IVDs.

Unfortunately modelling degeneration in the disc is problematic, and whilst collagenase digestion targets the collagen matrix within the disc the proteoglycan components would still be non-digested. However as the collagen matrix forms the interconnecting network which holds the proteoglycan proteins in place, it was observed that the majority of collagenase digested discs generated large voids both macro and microscopically mimicking at least in part morphological features of degeneration. A limitation of the current study was that digestion of the discs using collagenase did not always induce digestion (4 out of 10 discs) and these samples failed to show any mechanical response. Therefore when performing the hydrogel injection following collagenase digestion, discs were carefully examined to ensure voids were visible prior to hydrogel insertion. Following loading, histological analysis demonstrated collagenase digested voids were filled with hydrogel, in all discs investigated.

The reduced stiffness of collagenase digested discs and subsequent recovery following the introduction of the L-pNIPAM-co-DMAc hydrogel system may initially seem counter intuitive. Damage and degeneration of the NP expected to reduce 'fluid-like' behaviour of the disc in favour of stiffer, 'solid-like' behaviour [4,51,53]. The collagenase digestion process resulted in the creation of voids or fissures within the NP, as evidenced by macro and microscopic imaging of tissues, but minimal structural damage to the AF. The result, *in vitro*, is a disc which maintains its original height yet contains easily compressible voids, resulting in reduced bulk stiffness. More significant breakdown of disc tissue or full or partial excision of the disc nucleus, particularly when combined with long term, continuous pressure on the IVD *in vitro* [57] is liable to compress voids, reducing disc height and resulting in a thin disc of mostly AF tissue, which is stiffer than that of the NP [58]. This non-linear variation in disc stiffness with degeneration grade has previously been observed in torsion, flexion and bending [59,60]. When comparing stiffness of moderately degenerate discs compressed *in vitro* to degenerate discs *in vivo* it may be more accurate to look at the results in terms of potential to lose disc height, an important biomarker of disc degeneration [23–27].

Interestingly, significantly lower energy dissipation was observed in groups injected with the needle: sham injected; collagenase digested; and collagenase digestion followed by hydrogel injection, compared with healthy whole bovine IVDs. In contrast Michalek & Iatridis, (2012) observed no apparent difference in pressurization testing following needle puncture of bovine motion segments [61]. Interestingly however the study by Michalek & Iatridis (2012) induced a 10 mm deep defect within the AF which would not have led to puncture of the NP, unlike the current study where needle puncture was performed to the centre of the disc and thus into the NP region [61]. Furthermore the loading rate investigated by Michalek & Iatridis, (2012) was considerably lower (0.1 Hz) compared to the 2 Hz used in the present study [61]. In the present study these dynamic parameters were selected to mimic that of walking in the human spine to enable a functional assessment of the treatment methods. The loss in energy dissipation seen in the current study following needle puncture through the AF and into the NP together with the results of Carragee et al., 2009, suggests that the needle puncture itself in healthy IVDs may be the key initiator of discs losing tissue functionality, likely due to a loss in the pressure of the IVD [62]. However, as the degenerate human disc will already have a reduced energy dissipation capacity due to matrix degradation and presence of fissures [51,63,64]. The delivery of the L-pNIPAM-co-DMAc hydrogel system via needle injection, is not likely to initiate any further loss in energy dissipation but will provide an immediate mechanical and clinical benefit in terms of IVD stabilisation, to what is likely to be, at the time of patient treatment, a mechanically dysfunctional tissue.

The injection of acellular L-pNIPAM-co-DMAc hydrogel injection did not recover energy dissipation to pre-digested levels; however the energy dissipation functionality is reliant on the unique pressurised environment of the intact IVD [65], therefore it is unlikely that the implantation of a biomaterial alone would provide this biomechanical function immediately. It is hypothesised that over time as the L-pNIPAM-co-DMAc hydrogel integrates with surrounding NP tissue, whilst the delivered MSCs simultaneously repair and regenerate a biologically functioning NP matrix to fill in any potential fissures, that the pressurised environment and energy dissipation function of the IVD will be restored.

The mechanical benefit of hydrogel injection within IVDs has been previously reported, including the restoration of the load transmission [36] and re-established disc height maintained over 0.5 million loading cycles within a bovine organ culture model [15], however in both cases, nucleotomy was required for hydrogel implantation and the incorporation and delivery of cells was not investigated. Recently Balkovec et al., 2016 reported the restoration of segmental kinematics to pre injury state in IVDs with disc height loss, following hydrogel injection, within an *ex vivo* porcine cervical spine model; however again nucleotomy was required to inject the hydrogel, the incorporation and delivery of cells was not investigated [13] and the immediate mechanical restoration of the hydrogel was not maintained following cyclic loading [14].

The development of a biomaterial which offers the ability to safely deliver and differentiate cells, without the use of additional growth factors, as well as providing mechanical stabilisation, has so far not been achieved. Here, we demonstrate that the L-pNIPAM-co-DMAc hydrogel can be delivered by minimally invasive injection into collagenase digested whole bovine IVDs. Where it fills micro and macro fissures, is maintained within the disc during loading and provides immediate mechanical stabilisation with improved disc stiffness back to non-digested levels, without the need for prior removal of the NP tissue. Future investigations are required to assess the fatigue properties of the hydrogel following prolonged cyclic loading. The promising results displayed here suggest that the L-pNIPAM-co-DMAc hydrogel could provide a treatment strategy which requires a less invasive surgical intervention, in regards to removal of native tissue, which may promote better tissue integration and tissue functionality. Moreover the ability to safely deliver and promote NP differentiation of MSCs within the L-pNIPAM-co-DMAc hydrogel system also provides the opportunity to biologically repair the disc as well as providing mechanical stability.

4.3. Treatment design strategy tailored for stage of degeneration

Our improved understanding of the underlying pathogenesis of IVD degeneration over recent years and the consequential morphological changes that occur should be conveyed in our treatment design strategies [21,22]. It is possible that clinicians could be presented with a variety of treatment options, both cellular and acellular, in order to deliver the most efficacious, safe and cost effective treatment for the stage of degeneration [21]. Of course clinical translation is reliant on the detection and diagnosis of patients with early to mid-stages of IVD degeneration; however recent

advances in quantitative MRI imaging give future promise to this possibility [66]. Future investigations into the survival and differentiation of MSCs within the hostile environment of a severely degenerate IVD are crucial in determining the success of stem cell intervention for these patients. Additionally hydrogel containment and mechanical stability within severely degenerate IVDs, where annular fissures, osteophytes and endplate fractures may be clinically present, must also be investigated to assess whether hydrogels can offer clinical benefit for late stage IVD degeneration. The results of these investigations, in combination with the design of suitable biomaterials and diagnostic techniques will determine the future possibility of personalized therapies for IVD degeneration.

5. Conclusion

Here, we investigated the efficacy of a range of treatment options: hMSCS injected alone, acellular L-pNIPAM-co-DMAc and hMSCs incorporated within the L-pNIPAM-co-DMAc hydrogel, injected into bovine NP tissue explants. Demonstrating that hMSCs injected alone or incorporated within the L-pNIPAM-co-DMAc hydrogel are able to differentiate and produce NP matrix components, thus providing compelling evidence in support of cell delivery for NP matrix repair. Additionally we have demonstrated immediate mechanical stabilisation with the injection of acellular L-pNIPAM-co-DMAc hydrogel into whole bovine IVDs, demonstrating a potential clinical benefit even in the absence of cells. The delivery of the L-pNIPAM-co-DMAc hydrogel system via minimally invasive 26 gauge needle injection and its ability to fill micro fissures, without the removal of the existing NP tissue, provides the opportunity to target symptomatic patients in early to mid-stages of degeneration. The use of a combined cellular and mechanical repair approach is particularly promising since it is hypothesised that the L-pNIPAM-co-DMAc hydrogel, could restore disc height, thus providing immediate pain relief, whilst delivery of MSCs provides gradual regeneration.

Author contributions

AAT performed the majority of the laboratory work (except for the mechanical testing of whole bovine IVDs), data analysis and statistical analysis, contributed to study design and drafted the manuscript. GD performed the laboratory work and data analysis for the mechanical testing of whole bovine IVDs and helped draft the manuscript. LV assisted in the experimental set up of bovine NP tissue explants and critically revised the manuscript. NS and GC participated in the design and coordination of the mechanical testing experiments on whole bovine IVDs, aided in the analysis of data and critically revised the manuscript. CS and CLLM conceived the study, participated in its design and coordination, aided in the analysis of data, secured funding and critically revised the manuscript. All authors read and approved the final manuscript.

Disclosure

No conflicts of interest to declare.

Acknowledgements

We would like to offer kind thanks to the Biomolecular Sciences Research Centre, Sheffield Hallam University and Manchester Metropolitan University for PhD studentships. The Authors thank the EPSRC (EP/H000275/1, EP/1016473/1) for initial funding for this research and the Daphne Jackson for supporting Dr. Louise Vickers as a Daphne Jackson postdoctoral fellow.

Appendix A. Supplementary data

Supplementary data associated with this article can be found, in the online version, at http://dx.doi.org/10.1016/j.actbio.2017.03.010.

References

[1] D.G. Hoy, E. Smith, M. Cross, L. Sanchez-Riera, F.M. Blyth, R. Buchbinder, A.D. Woolf, T. Driscoll, P. Brooks, L.M. March, Reflecting on the global burden of musculoskeletal conditions: lessons learnt from the global burden of disease 2010 study and the next steps forward, Ann. Rheum. Dis. 74 (2015) 4–7.
[2] K.M. Cheung, J. Karppinen, D. Chan, D.W. Ho, Y.Q. Song, P. Sham, K.S. Cheah, J.C. Leong, K.D. Luk, Prevalence and pattern of lumbar magnetic resonance imaging changes in a population study of one thousand forty-three individuals, Spine (Phila Pa 1976) 34 (2009) 934–940.
[3] G. Livshits, M. Popham, I. Malkin, P.N. Sambrook, A.J. Macgregor, T. Spector, F. M. Williams, Lumbar disc degeneration and genetic factors are the main risk factors for low back pain in women: the UK Twin Spine Study, Ann. Rheum. Dis. 70 (2011) 1740–1745.
[4] P.J. Roughley, Biology of intervertebral disc aging and degeneration: involvement of the extracellular matrix, Spine 29 (2004) 2691–2699.
[5] A. Schultz, D. Warwick, M. Berkson, A. Nachemson, Mechanical properties of human lumbar spine motion segments—Part I: Responses in flexion, extension, lateral bending, and torsion, J. Biomech. Eng. 101 (1979) 46–52.
[6] C. Le Maitre, A. Pockert, D. Buttle, A. Freemont, J. Hoyland, Matrix synthesis and degradation in human intervertebral disc degeneration, Biochem. Soc. Trans. 35 (2007) 652.
[7] G. Cs-Szabo, D. Ragasa-San Juan, V. Turumella, K. Masuda, E.J. Thonar, H.S. An, Changes in mRNA and protein levels of proteoglycans of the anulus fibrosus and nucleus pulposus during intervertebral disc degeneration, Spine (Phila Pa 1976) 27 (2002) 2212–2219.
[8] J.A. Hoyland, C. Le Maitre, A.J. Freemont, Investigation of the role of IL-1 and TNF in matrix degradation in the intervertebral disc, Rheumatology (Oxford) 47 (2008) 809–814.
[9] C.L. Le Maitre, J.A. Hoyland, A.J. Freemont, Catabolic cytokine expression in degenerate and herniated human intervertebral discs: IL-1beta and TNFalpha expression profile, Arthritis Res. Ther. 9 (2007) R77.
[10] C.L. Le Maitre, A.J. Freemont, J.A. Hoyland, Accelerated cellular senescence in degenerate intervertebral discs: a possible role in the pathogenesis of intervertebral disc degeneration, Arthritis Res. Ther. 9 (2007) R45.
[11] J.P. Urban, J.F. McMullin, Swelling pressure of the lumbar intervertebral discs: influence of age, spinal level, composition, and degeneration, Spine (Phila Pa 1976) 13 (1988) 179–187.
[12] K. Olmmarker, B. Rydevik, Single-versus double-level nerve root compression: an experimental study on the porcine cauda equina with analyses of nerve impulse conduction properties, Clin. Orthop. 279 (1992) 35–39.
[13] C. Balkovec, A.J. Vernengo, S.M. McGill, Disc height loss and restoration via injectable hydrogel influences adjacent segment mechanics in-vitro, Clin. Biomech. 36 (2016) 1–7.
[14] C. Balkovec, A.J. Vernengo, P. Stevenson, S.M. McGill, Evaluation of an injectable hydrogel and polymethyl methacrylate in restoring mechanics to compressively fractured spine motion segments, Spine J. 11 (2016) 1404–1412.
[15] A. Schmocker, A. Khoushabi, D.A. Frauchiger, B. Gantenbein, C. Schizas, C. Moser, P. Bourban, D.P. Pioletti, A photopolymerized composite hydrogel and surgical implanting tool for a nucleus pulposus replacement, Biomaterials 88 (2016) 110–119.
[16] D. Miles, E. Mitchell, N. Kapur, P. Beales, R. Wilcox, Peptide: glycosaminoglycan hybrid hydrogels as an injectable intervention for spinal disc degeneration, J. Mater. Chem. B 4 (2016) 3225–3231.
[17] C.L. Le Maitre, P. Baird, A.J. Freemont, J.A. Hoyland, An in vitro study investigating the survival and phenotype of mesenchymal stem cells following injection into nucleus pulposus tissue, Arthritis Res. Ther. 11 (2009) R20.
[18] K.W. Kim, T.H. Lim, J.G. Kim, S.T. Jeong, K. Masuda, H.S. An, The origin of chondrocytes in the nucleus pulposus and histologic findings associated with the transition of a notochordal nucleus pulposus to a fibrocartilaginous nucleus pulposus in intact rabbit intervertebral discs, Spine (Phila Pa 1976) 28 (2003) 982–990.
[19] L. Orozco, R. Soler, C. Morera, M. Alberca, A. Sanchez, J. Garcia-Sancho, Intervertebral disc repair by autologous mesenchymal bone marrow cells: a pilot study, Transplantation 92 (2011) 822–828.
[20] Y. Zhang, X. Guo, P. Xu, L. Kang, J. Li, Bone mesenchymal stem cells transplanted into rabbit intervertebral discs can increase proteoglycans, Clin. Orthop. 430 (2005) 219–226.
[21] A. Thorpe, C. Sammon, C. Le Maitre, Cell or not to cell'that is the question: for intervertebral disc regeneration, J. Stem Cell. Res. Dev. 2 (2015).
[22] C.L. Le Maitre, A.L. Binch, A.A. Thorpe, S.P. Hughes, Degeneration of the intervertebral disc with new approaches for treating low back pain, J. Neurosurg. Sci. 59 (2015) 47–61.
[23] A. Thorpe, V. Boyes, C. Sammon, C. Le Maitre, Thermally triggered injectable hydrogel, which induces mesenchymal stem cell differentiation to nucleus

pulposus cells: potential for regeneration of the intervertebral disc, Acta Biomater. 36 (2016) 99–111.
[24] S.M. Richardson, N. Hughes, J.A. Hunt, A.J. Freemont, J.A. Hoyland, Human mesenchymal stem cell differentiation to NP-like cells in chitosan–glycerophosphate hydrogels, Biomaterials 29 (2008) 85–93.
[25] D. Kumar, I. Gerges, M. Tamplenizza, C. Lenardi, N.R. Forsyth, Y. Liu, Three-dimensional hypoxic culture of human mesenchymal stem cells encapsulated in a photocurable, biodegradable polymer hydrogel: a potential injectable cellular product for nucleus pulposus regeneration, Acta Biomater. 8 (2014) 3463–3467.
[26] G. Vadalà, G. Sowa, M. Hubert, L.G. Gilbertson, V. Denaro, J.D. Kang, Mesenchymal stem cells injection in degenerated intervertebral disc: cell leakage may induce osteophyte formation, J. Tissue Eng. Regen. Med. 6 (2012) 348–355.
[27] F.L. Acosta Jr., L. Metz, H.D. Adkisson IV, J. Liu, E. Carruthers-Liebenberg, C. Milliman, M. Maloney, J.C. Lotz, Porcine intervertebral disc repair using allogeneic juvenile articular chondrocytes or mesenchymal stem cells, Tissue Eng. Part A 17 (2011) 3045–3055.
[28] H. Serhan, D. Mhatre, H. Defossez, C.M. Bono, Motion-preserving technologies for degenerative lumbar spine: the past, present, and future horizons, SAS J. 5 (2011) 75–89.
[29] M. Pelletier, W. Walsh, N. South, Nucleus replacement, Biomater 171 (2011) e190.
[30] S. Holm, A.K. Holm, L. Ekstrom, A. Karladani, T. Hansson, Experimental disc degeneration due to endplate injury, J. Spinal Disord. Tech. 17 (2004) 64–71.
[31] A.J. Michalek, M.R. Buckley, L.J. Bonassar, I. Cohen, J.C. Iatridis, The effects of needle puncture injury on microscale shear strain in the intervertebral disc annulus fibrosus, Spine J. 10 (2010) 1098–1105.
[32] C.L. Le Maitre, A.J. Freemont, J.A. Hoyland, The role of interleukin-1 in the pathogenesis of human intervertebral disc degeneration, Arthritis Res. Ther. 7 (2005) R732–R745.
[33] A.A. Thorpe, S. Creasey, C. Sammon, C.L. Le Maitre, Hydroxyapatite nanoparticle injectable hydrogel scaffold to support osteogenic differentiation of human mesenchymal stem cells, Eur. Cell Mater. 32 (2016) 1–23.
[34] D. Kumar, A.M. Lyness, I. Gerges, C. Lenardi, N.R. Forsyth, Y. Liu, Stem cell delivery with polymer hydrogel for treatment of intervertebral disc degeneration: from 3D culture to design of the delivery device for minimally invasive therapy, Cell Transplant. 25 (12) (2016) 2213–2220.
[35] M.H. Amer, L.J. White, K.M. Shakesheff, The effect of injection using narrow-bore needles on mammalian cells: administration and formulation considerations for cell therapies, J. Pharm. Pharmacol. 67 (2015) 640–650.
[36] Z. Zhou, M. Gao, F. Wei, J. Liang, W. Deng, X. Dai, G. Zhou, X. Zou, Shock absorbing function study on denucleated intervertebral disc with or without hydrogel injection through static and dynamic biomechanical tests in vitro, Biomed. Res. Int. 2014 (2014) 461724.
[37] Z. Li, G. Lamg, X. Chen, H. Sacks, C. Mantzur, U. Tropp, K.T. Mader, T.C. Smallwood, C. Sammon, G. Richards, M. Alini, S. Grad, Polyurethane scaffold with in situ swelling capacity for nucleus pulposus replacement, Biomaterials 84 (2016) 196–209.
[38] A. Hiyama, J. Mochida, T. Iwashina, H. Omi, T. Watanabe, K. Serigano, F. Tamura, D. Sakai, Transplantation of mesenchymal stem cells in a canine disc degeneration model, J. Orthop. Res. 26 (2008) 589–600.
[39] D. Sakai, J. Mochida, T. Iwashina, A. Hiyama, H. Omi, M. Imai, T. Nakai, K. Ando, T. Hotta, Regenerative effects of transplanting mesenchymal stem cells embedded in atelocollagen to the degenerated intervertebral disc, Biomaterials 27 (2006) 335–345.
[40] C. Malonzo, S. Chan, A. Kabiri, D. Eglin, S. Grad, H. Bonél, L. Benneker, B. Gantenbein-Ritter, A papain-induced disc degeneration model for the assessment of thermo-reversible hydrogel–cells therapeutic approach, J. Tissue Eng. Regen. Med. 9 (2015) E167–E176.
[41] G. Crevensten, A.J. Walsh, D. Ananthakrishnan, P. Page, G.M. Wahba, J.C. Lotz, S. Berven, Intervertebral disc cell therapy for regeneration: mesenchymal stem cell implantation in rat intervertebral discs, Ann. Biomed. Eng. 32 (2004) 430–434.
[42] F. Mwale, H.T. Wang, P. Roughley, J. Antoniou, L. Haglund, Link N and mesenchymal stem cells can induce regeneration of the early degenerate intervertebral disc, Tissue Eng. Part A 20 (2014) 2942–2949.
[43] C. Neidlinger-Wilke, F. Galbusera, H. Pratsinis, E. Mavrogonatou, A. Mietsch, D. Kletsas, H. Wilke, Mechanical loading of the intervertebral disc: from the macroscopic to the cellular level, Eur. Spine J. 23 (2014) 333–343.
[44] J.P. Urban, S. Smith, J.C. Fairbank, Nutrition of the intervertebral disc, Spine 29 (2004) 2700–2709.
[45] S. Reitmaier, L. Kreja, K. Gruchenberg, B. Kanter, J. Silva-Correia, J.M. Oliveira, R. L. Reis, V. Perugini, M. Santin, A. Ignatius, H.J. Wilke, In vivo biofunctional evaluation of hydrogels for disc regeneration, Eur. Spine J. 23 (2014) 19–26.
[46] H.N. Fernando, J. Czamanski, T. Yuan, W. Gu, A. Salahadin, C.C. Huang, Mechanical loading affects the energy metabolism of intervertebral disc cells, J. Orthop. Res. 29 (2011) 1634–1641.
[47] J.C. Iatridis, J.J. MacLean, P.J. Roughley, M. Alini, Effects of mechanical loading on intervertebral disc metabolism in vivo, J. Bone Joint Surg. Am. 88 (Suppl 2) (2006) 41–46.
[48] J. Dai, H. Wang, G. Liu, Z. Xu, F. Li, H. Fang, Dynamic compression and co-culture with nucleus pulposus cells promotes proliferation and differentiation of adipose-derived mesenchymal stem cells, J. Biomech. 47 (2014) 966–972.
[49] B. Gantenbein, S. Illien-Jünger, C.W. Chan, J. Walser, L. Haglund, J.S. Ferguson, J. C. Iatridis, S. Grad, Organ culture bioreactors-platforms to study human intervertebral disc degeneration and regenerative therapy, Curr. Stem Cell Res. Ther. 10 (2015) 339–352.
[50] J.C. Iatridis, M. Weidenbaum, L.A. Setton, V.C. Mow, Is the nucleus pulposus a solid or a fluid? Mechanical behaviors of the nucleus pulposus of the human intervertebral disc, Spine 21 (1996) 1174–1184.
[51] J.C. Iatridis, L.A. Setton, M. Weidenbaum, V.C. Mow, Alterations in the mechanical behavior of the human lumbar nucleus pulposus with degeneration and aging, J. Orthop. Res. 15 (1997) 318–322.
[52] P.J. Roughley, L.I. Melching, T.F. Heathfield, R.H. Pearce, J.S. Mort, The structure and degradation of aggrecan in human intervertebral disc, J. Orthop. Res. 15 (2006) 326–332.
[53] J.I. Boxberger, S. Sen, C.S. Yerramalli, D.M. Elliott, Nucleus pulposus glycosaminoglycan content is correlated with axial mechanics in rat lumbar motion segments, J. Orthop. Res. 24 (2006) 1906–1915.
[54] J. Silva-Correia, A. Gloria, M.B. Oliveira, J.F. Mano, J.M. Oliveira, L. Ambrosio, R.L. Reis, Rheological and mechanical properties of acellular and cell-laden methacrylated gellan gum hydrogels, J. Biomed. Mater. Res. A 101 (2013) 3438–3446.
[55] J. Silva-Correia, J.M. Oliveira, S. Caridade, J.T. Oliveira, R. Sousa, J. Mano, R. Reis, Gellan gum-based hydrogels for intervertebral disc tissue-engineering applications, J. Tissue Eng. Regen. Med. 5 (2011) e97–e107.
[56] B.G. van Dijk, E. Potier, K. Ito, Long-term culture of bovine nucleus pulposus explants in a native environment, Spine J. 13 (2013) 454–463.
[57] K. Sato, S. Kikuchi, T. Yonezawa, In vivo intradiscal pressure measurement in healthy individuals and in patients with ongoing back problems, Spine 24 (1999) 2468.
[58] D. Périé, D. Korda, J.C. Iatridis, Confined compression experiments on bovine nucleus pulposus and annulus fibrosus: sensitivity of the experiment in the determination of compressive modulus and hydraulic permeability, J. Biomech. 38 (2005) 2164–2171.
[59] M.A. Adams, P. Dolan, W.C. Hutton, The stages of disc degeneration as revealed by discograms, J. Bone Joint Surg. Br. 68 (1986) 36–41.
[60] W. Frobin, P. Brinckmann, M. Kramer, E. Hartwig, Height of lumbar discs measured from radiographs compared with degeneration and height classified from MR images, Eur. Radiol. 11 (2001) 263–269.
[61] A.J. Michalek, J.C. Iatridis, Height and torsional stiffness are most sensitive to annular injury in large animal intervertebral discs, Spine J. 12 (5) (2012) 425–432.
[62] E.J. Carragee, A.S. Don, E.L. Hurwitz, J.M. Cuellar, J.A. Carrino, R. Herzog, 2009 ISSLS Prize Winner: does discography cause accelerated progression of degeneration changes in the lumbar disc: a ten-year matched cohort study, Spine (Phila Pa 1976) 34 (2009) 2338–2345.
[63] W. Koeller, S. Muehlhaus, W. Meier, F. Hartmann, Biomechanical properties of human intervertebral discs subjected to axial dynamic compression—influence of age and degeneration, J. Biomech. 19 (1986) 807–816.
[64] L.A. Setton, J. Chen, Mechanobiology of the intervertebral disc and relevance to disc degeneration, J. Bone Joint Surg. Am. 88 (Suppl 2) (2006) 52–57.
[65] W. Koeller, W. Meier, F. Hartmann, Biomechanical properties of human intervertebral discs subjected to axial dynamic compression. A comparison of lumbar and thoracic discs, Spine (Phila Pa 1976) 9 (1984) 725–733.
[66] M. Brayda-Bruno, M. Tibiletti, K. Ito, J. Fairbank, F. Galbusera, A. Zerbi, S. Roberts, E. Wachtel, Y. Merkher, Advances in the diagnosis of degenerated lumbar discs and their possible clinical application, Eur. Spine J. 23 (2014) 315–323.